Reconfiguring Steel Structures:

Energy Dissipation and Buckling Mitigation Through the Use of Steel Foams

Principal Investigators:
Sanjay R. Arwade (University of Massachusetts)
Jerome F. Hajjar (Northeastern University)
Benjamin W. Schafer (Johns Hopkins University)

Technical Report 12-01

Cell ligament stiffness, geometric uncertainty, and the elastic properties of cellular networks

Authors:
Sanjay R. Arwade, University of Massachusetts, Amherst
Benjamin W. Schafer, Johns Hopkins University

Date: January 14, 2012

Grants: CMMI-1000334, CMMI-1000167, CMMI-0970059

NSF CMMI-1000334, 1000167, 0970059 — Technical Report 12-01 — January 2012

Cell ligament stiffness, geometric uncertainty, and the elastic properties of cellular networks

Sanjay R. Arwade[1] & Benjamin W. Schafer[2]

1. Corresponding author: 223 Marston Hall, Dept. of Civil & Env. Engg.
University of Massachusetts,
Amherst, MA, 01003, USA arwade@ecs.umass.edu

2. 203 Latrobe Hall, Dept. of Civil Engg., Johns Hopkins University,
Baltimore, MD, 21218, USA schafer@jhu.edu

Abstract: The objective of this paper is to examine the sensitivity of the properties of cellular networks to the axial-to-bending stiffness ratio of the walls of the inter-connected network. Cellular networks are the underlying load-bearing system of a large number of materials and structures. Analytical expressions are provided for the effective elastic properties as well as the density as a function of the axial-to-bending stiffness ratio. It is shown that the effective elastic properties are sensitive to the axial-to-bending stiffness ratio in structuraly relevant regimes. It is also shown that the density of the cellular network does not uniquely define the observed variations in elastic properties, and that cellular networks with the same density may have substantially different elastic properties due to differences in the axial-to-bending stiffness ratio. Finally, through simulation the sensitivity and accuracy of the derived effective property expressions is explored for networks which are per-

turbed from perfect topologies, and it is shown that the properties of cellular networks with perturbed topology differ from those predicted by expressions based on periodic cellular networks.

keywords: honeycombs, foams, mechanical properties, uncertainty, Monte Carlo simulation

1 Introduction

The use of structural cellular networks (See Fig. 1 for some examples) is now common in a variety of engineering applications such as packaging, energy absorption and aerospace structures, and the mechanics of such materials, generally called cellular networks, are largely well understood and documented (5). Cellular networks also represent a potentially convenient means to approximate other complicated inter-connected assemblages of members, whether they be biological such as the actin filament networks that exist in the cytoskeleton of living cells (Fig. 1a), or man-made such as the interconnected steel members of a high-rise buidling or transmission tower (Fig. 1c). In any of these cases knowledge of the effective elastic properties can aid both prediction of key behavior and design of the resulting structure (or material).

A broad set of assumptions, including that cell walls are solid and rectangular in cross section, that the cell geometry is periodic, that material defor-

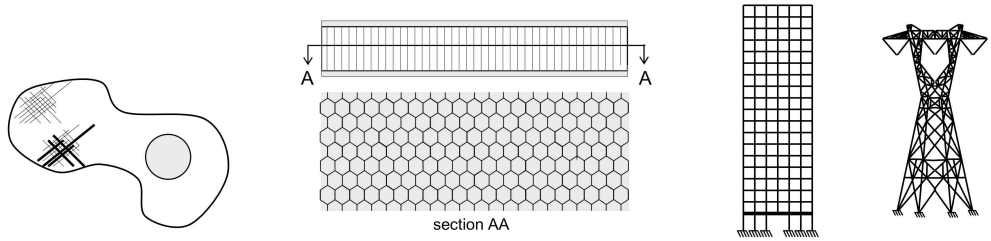

(a) Actin filament networks in the cytoskeleton of a cell

(b) Metallic honeycomb network in a sandwich panel

(c) Structural networks of steel members in buildings and towers

Figure 1: Some typical cellular networks occurring in natural and engineered systems from the nano- to macro-scale

mation is dominated by bending of the cell walls, and that relative density determines the elastic properties of the material allow prediction of the elastic properties of cellular networks using relatively simple analytical expressions. This paper describes how relaxing the assumptions of solid, rectangular cell walls affects the elastic properties of two dimensional cellular networks, and how breaking the periodicity of the cells in two dimensional cellular networks affects the ability to accurately predict the elastic properties. In addition to these topics, this paper also adapts expressions for the elastic properties of cellular networks to depend on ratios of the bending and axial stiffness of the cell walls. When combined with a survey of the axial-to-bending stiffness ratios of various structural, nanomechanical, and biological components, these new expressions provide insight into the dramatic range of properties that can be obtained by proper design of cellular microstructures.

This work has several sources of inspiration, and relies on a substan-

tial body of previous research into the mechanical properties of cellular networks. Extensive previous work on the elastic properties of two and three dimensional cellular networks have provided a broad array of tools to link the microstructure of the cellular network to the macroscopic properties (16; 6; 7; 21; 20). Some of these studies have indicated that even for disordered networks the elastic properties of the network can be predicted in an average sense by using a periodic unit cell approach. Although the studies have considered cell ligaments with variable cross section, they have all assumed that the ligaments have solid cross section, an assumption that is relaxed in the current work. The post-elastic response of cellular networks in compression has also been the subject of significant prior investigation (9; 12; 13; 17; 11) that has largely succeeded in defining the relationship between micromechanical phenomena such as cell ligament buckling and contact and macroscopic material response such as yielding and densification.

Preliminary investigations by the authors indicated that two dimensional cellular networks with identical relative density could have different effective elastic properties if the size of the cells and cross-sectional properties of the cell walls were controlled in particular ways (15). These results largely drove the current investigation into how the axial-to-bending stiffness ratio of the cell walls affects cellular network properties. Although cellular networks are predominantly available with only solid rectangular cross section walls, analytical studies have shown that exciting new materials can be envisioned and designed when the elements of a cellular network are made of elements

with cylindrical cross section (22). One of the author's previous research into the effect of uncertainty in the geometry of material microstructures on material response (4; 8; 18) drove the uncertainty characterization parts of this work, while work by the other author on the mechanics of thin-walled structures (see, among many others, (14)) and bio-chemical filaments (19) allows the determination of limits on realistic values for the axial-to-bending stiffness ratios used in predicting celular network properties. The basis of this contribution is the seminal work on the mechanics of cellular networks in which it was shown that unit cell approaches combined with a strength of materials approach to the response of cellular networks can yield accurate predictions of effective properties (5).

The paper begins with a review of cellular networks and defines the geometry of the materials under consideration along with the notation used to describe this geometry. From the geometry definitions come the definition of the axial-to-bending stiffness ratios of the cell walls, used throughout the paper as the key parameters in describing the network microstructure. For practical engineered or naturally occurring materials, these axial-to-bending stiffness ratios can exist only over a certain range of values, which is illustrated by the calculation of the axial-to-bending stiffness ratios for a variety of structural and bio-chemical elements. A new relationship is also developed that relates the relative density to the axial-to-bending stiffness ratios for a variety of possible cell wall cross sectional geometries. Next, the effective elastic properties of two dimensional cellular networks are expressed as func-

tions of the axial-to-bending stiffness ratios, and it is shown that relative density does not provide a unique prediction of cellular network properties in all cases. Finally, Monte Carlo simulation is used to investigate the effect of irregularity of the cell geometry on network properties.

2 Cellular Networks

The typical two dimensional cellular network is a honeycomb composed of hexagonal cells divided by cell walls of solid material. These networks are often periodic, allowing analysis of their mechanics by examination of a single unit cell of the network. This section introduces the notation used to define the geometry of the unit cell and the cross-sectional properties of the cell walls, and then defines ratios of the axial to bending stiffness of the cell walls that will be used in later computation of the effective properties.

2.1 Unit cell notation

A unit cell is pictured in Fig. 2 with the geometric notation used in this paper. The geometry of the unit cell is defined by the length h of the upright wall, the length l of the oblique wall, and the angle θ which defines the included angles of the hexagons. The unit cell is a regular hexagon when $h = l$ and $\theta = \pi/6$, is a rectangle with aspect ratio of 2 when $h = l$ and $\theta = 0$, and is a square when $h = 2l$ and $\theta = 0$. When $\theta < 0$ the unit cell becomes non-convex, and interesting properties are obtained.

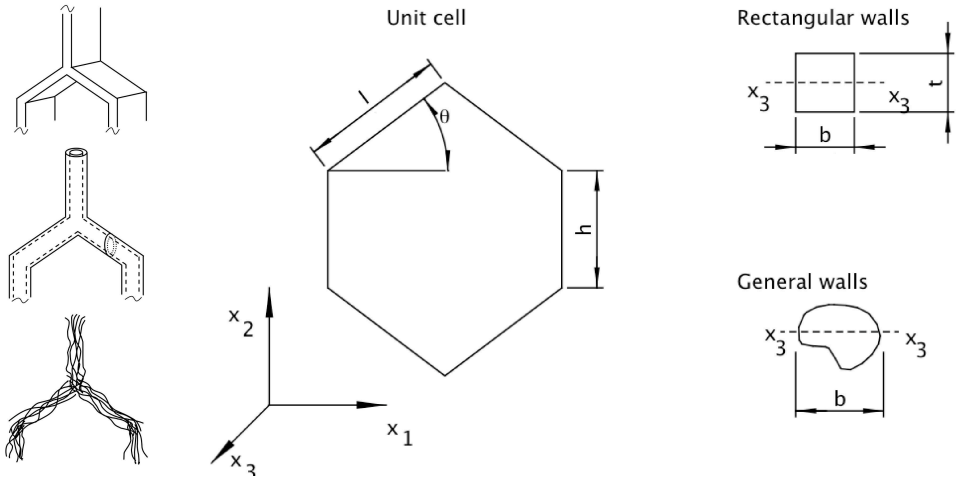

Figure 2: The unit cell of a hexagonal cellular network. On the right are shown a rectangular and general wall cross section, and on the left are show some possible cell wall structures–solid rectangles, hollow tubes, and bundles of filaments.

In traditional treatments of the mechanics of cellular networks, the cell wall geometry is defined by the cell wall thickness t, and the geometry is assumed to independent of the out-of-plane x_3 coordinate so that unit thickness $b = 1$ can be arbitrarily assigned to the out-of-plane dimension. One of the main goals of this work is to examine the effect on the mechanical properties when the assumption of rectangular cell walls is relaxed. Herein, therefore, the cell wall properties are defined by the cross sectional area A and the second moment of inertia I. The moment of inertia used here is that governing the in-plane bending stiffness of the cell walls.

Furthermore, the upright and oblique members may in general have different cross sections, defined by A_h and I_h for the upright members and A_l and I_l for the oblique members.

2.2 Stiffness ratios

The cell wall areas and moment of inertias, combined with the lengths of the cell walls lead to the axial stiffness of the cell walls

$$\begin{aligned} K_{ah} &= \frac{E_s A_h}{h} \\ K_{al} &= \frac{E_s A_l}{l} \end{aligned} \tag{1}$$

and the bending stiffness of the cell walls

$$\begin{aligned} K_{bh} &= \frac{12 E_s I_h}{h^3} \\ K_{bl} &= \frac{12 E_s I_l}{l^3} \end{aligned} \tag{2}$$

where E_s is the elastic modulus of the isotropic elastic material of which the network is composed and the bending stiffness term has been chosen to best represent the type of bending deformation that occurs in the cell walls, and because this choice of bending stiffness has the same dimensions as the axial stiffness, force divided by length (rendering R_k nondimensional).

The ratio of the axial to bending stiffness is then defined to be, for the upright and oblique elements respectively,

$$\begin{aligned} R_{kh} &= \frac{K_{ah}}{K_{bh}} = \frac{A_h h^2}{12 I_h} \\ R_{kl} &= \frac{K_{al}}{K_{bl}} = \frac{A_l l^2}{12 I_l}, \end{aligned} \tag{3}$$

and the ratio of the bending stiffnesses of the cell walls is

$$R_b = \frac{K_{bl}}{K_{bh}} = \frac{I_l}{I_h}\left(\frac{h}{l}\right)^3 \tag{4}$$

3 Axial-to-bending stiffness ratios (R_k) for cellular networks

This section examines the axial-to-bending stiffness ratio for cellular networks, first providing the analytical expressions as a function of the geometry of the walls and then examining the axial-to-bending stiffness ratio for a variety of existing networks. Finally the dependence of the relationship between density and axial-to-bending stiffness is explored as a function of the wall cross-section geometry.

3.1 R_k dependence on wall geoemetry

For a given wall cross-section Eqs. 3 and 4 may be simplified. For example, in the special (classical) case when the cell walls are rectangular in cross section and the in-plane thickness of the upright and oblique walls is the same (t)

these expressions reduce to

$$\begin{aligned} R_{kh} &= \left(\frac{h}{t}\right)^2 \\ R_{kl} &= \left(\frac{l}{t}\right)^2 \\ R_b &= \left(\frac{h}{l}\right)^3 . \end{aligned} \tag{5}$$

Note, the definition for R_b applies to any cross-section where the upright and oblique walls have the same cross-section.

Another case of interest, is that of a network comprised of hollow tubes. For an oblique wall comprised of a hollow component with circular cross-section, outside diameter d_o and diameter-to-thickness ratio D,

$$R_{kl} = 2/3\left(\frac{D^2}{D^2 - 2D + 2}\right)\left(\frac{l}{d_o}\right)^2 . \tag{6}$$

In the limit as $D \to \infty$

$$R_{kl} = 2/3\left(\frac{l}{d_o}\right)^2 . \tag{7}$$

or in the limit for a solid wall $D = 2$ and

$$R_{kl} = 4/3\left(\frac{l}{d_o}\right)^2 . \tag{8}$$

3.2 R_k ranges for cellular networks

In the limit as h or l are increased the axial-to-bending stiffness ratio (R_k) approaches ∞ and axial deformations may be ignored in the network. Given the remarkably wide range of scales and applications for which networks exist, what ranges of R_k are typically expected? In Table 1 the axial-to-bending stiffness ratio for a wide variety of different natural and engineered networks is explored.

From a practical standpoint R_k in cellular networks may be summarized as follows: $R_k < 10^0$ atypical/infeasible, $10^0 < R_k < 10^1$ rare, $10^1 < R_k < 10^2$ most common, $10^2 < R_k < 10^3$ common, $R_k > 10^3$ possible, but rare. These ranges provide a general means for exploring the sensitivity of the effective properties to R_k.

4 Effective Properties

A periodic cellular network for which a unit cell exists has effective elastic properties that are orthotropic and are defined by the compliance matrix

$$C* = \begin{bmatrix} \frac{1}{E_1^*} & -\frac{\nu_{21}^*}{E_2^*} & 0 \\ -\frac{\nu_{12}^*}{E_1^*} & \frac{1}{E_2^*} & 0 \\ 0 & 0 & \frac{1}{2G_{12}^*} \end{bmatrix}. \tag{9}$$

The classical solution for the four effective elastic constants E_1^*, E_2^*, ν_{12}^*, ν_{21}^* and G_{12}^* assumes rectangular cross sectional walls and hexagonal unit

Table 1: Axial-to-bending stiffness ratio (R_k) for different networks elements

type of network	R_k min	R_k max
nanoscale biological network[1]		
single actin filaments	$1.6 * 10^2$	$1.6 * 10^4$
bundles of 19 actin filaments	$5.1 * 10^0$	$5.1 * 10^2$
nanoscale material		
carbon nanotubes [2]	$1.3 * 10^1$	$5.0 * 10^1$
mesoscale material		
walls of metallic foams [3]	$1.7 * 10^0$	$3.3 * 10^3$
macroscale structural system		
steel pipe in a space truss[4]	$1.0 * 10^0$	$2.4 * 10^1$

Table Notes
[1] Consider actin filaments as found in the cytoskeleton of living cells, or 19 closely packed actin filaments with base filaments and length the same as before, fully bonded (19)
[2] Consider a network of nanotubes where the components are single wall nanotubes, centerlined diameter of 1.6 nm, thickness of 0.34 nm, length from 7 to 14 nm. (10)
[3] Consider the reported range of $2 * 10^{-2} < \rho_n < 0.8$ on Al foams in Gibson (3) and Ashby and use Eq. 18 to provide the bounds
[4] Consider a space truss comprised of steel pipe with O.D. of 20 in., thickness from 1/8 to 1/2 in., and length from 2 to 10 ft. (2)

cells. Here these expressions are rewritten first to depend explicitly on the axial and bending stiffness of the cell walls, and then on the axial-to-bending stiffness ratios of the cell walls. Note that the expressions here account for bending and axial deformation of the cell walls but not shearing deformations.

Expressions for the properties in terms of the axial-to-bending stiffness ratios are

$$
\begin{aligned}
E_1^* &= \frac{K_{bl}\cos\theta}{b(\frac{h}{l}+\sin\theta)\left(\sin^2\theta+\frac{\cos^2\theta}{R_{kl}}\right)} \\
E_2^* &= \frac{(\frac{h}{l}+\sin\theta)K_{bl}}{b\cos\theta\left(\cos^2\theta+\frac{\sin^2\theta}{R_{kl}}+2\frac{R_b}{R_{kh}}\right)} \\
\nu_{12}^* &= \frac{\left(1-\frac{1}{R_{kl}}\right)\sin\theta\cos^2\theta}{(\frac{h}{l}+\sin\theta)\left(\sin^2\theta+\frac{\cos^2\theta}{R_{kl}}\right)} \\
\nu_{21}^* &= \frac{\left(1-\frac{1}{R_{kl}}\right)(\frac{h}{l}+\sin\theta)\sin\theta}{\cos^2\theta+\frac{\sin^2\theta}{R_{kl}}+2\frac{R_b}{R_{kh}}} \\
G_{12}^* &= \frac{(\frac{h}{l}+\sin\theta)K_{bl}}{b\left(2\cos\theta R_b+\left(\frac{h}{l}\right)^2\cos\theta+\frac{1}{2R_{kl}\cos\theta}\right)}.
\end{aligned}
\tag{10}
$$

Note that the effective elastic and shear moduli retain the stiffness term K_{bl} in the numerator, indicating that the properties are not fully determined by the axial-to-bending stiffness ratios. The presence of this term prevents the ready normalization of the stiffness properties by E_s the solid elastic modulus, as is commonly done in the standard solutions. Although the expressions are not particularly compact, a solid-normalized set of stiffnesses can still be defined

by

$$\begin{aligned} \tilde{E}_1 &= \frac{E_1^*}{E_s} \\ \tilde{E}_2 &= \frac{E_2^*}{E_s} \\ \tilde{G}_{12} &= \frac{G_{12}^*}{G_s} \end{aligned} \tag{11}$$

These solid-normalized properties will be useful in investigating the effect of topological disorder and relative density on the elastic properties of cellular networks.

In addition to the solid-normalzied properties defined above, the components of the constitutive matrix can be normalized by $C' = \frac{C^*}{C_b}$ with $C_b = \lim_{R_{kh},R_{kl}\to\infty} C$ to obtain bending-normalized properties. That is, C_b is the constitutive matrix obtained from the consideration of only bending deformation of the cell walls. The bending-normalized effective properties

are

$$
\begin{aligned}
E'_1 &= \left[1 + \frac{1}{R_{kl}\tan^2\theta}\right]^{-1} \\
E'_2 &= \left[1 + \frac{\tan^2\theta}{R_{kl}} + \frac{2R_b}{R_{kh}\cos^2\theta}\right]^{-1} \\
\nu'_{12} &= \frac{1 - 1/R_{kl}}{1 + 1/R_{kl}\tan^2\theta} \\
\nu'_{21} &= \frac{1 - 1/R_{kl}}{1 + \frac{\tan^2\theta}{R_{kl}} + \frac{2R_b}{R_{kh}\cos^2\theta}} \\
G'_{12} &= \frac{2R_b + \left(\frac{h}{l}\right)^2}{2R_b + \left(\frac{h}{l}\right)^2 + \frac{1}{2R_{kl}\cos^2\theta}}.
\end{aligned}
\tag{12}
$$

This normalization allows the direct interpretation of the effect of axial deformations on the effective properties of cellular networks, which is a primary benefit of the introduction of the axial-to-bending stiffness ratio into the expressions. For example, E'_1 is only a function of the geometry θ and the axial-to-bending stiffness ratio R_{kl}. However, in general, the effective properties and the bending-normalized effective properties depend on the parameters R_{kh}, R_{kl}, R_b, K_{bl}, θ, (h/l), and b. This is a large parameter set that is difficult to investigate completely. In the next section, therefore, some special geometric cases are introduced that simplify the parameter space and allow easier interpretation of the effective property expressions.

5 Special geometric cases

In this section two special cases of the cellular network geometry are examined. In the first regular hexagonal cells are obtained by setting $\theta = \pi/6$ and in the second rectangular cells are obtained by $\theta = 0$. In both cases the upright and oblique cell walls are assumed to be identical with $h = l$, $I_h = I_l$, and $A_h = A_l$.

5.1 Regular hexagonal unit cell

When the substitutions to obtain regular hexagonal cells with identical cell walls are made to Eqs. 10 the expressions for the effective properties become

$$\begin{aligned} E_1^* = E_2^* = E^* &= \frac{4K_b}{b\sqrt{3}\left(1+\frac{3}{R_k}\right)} \\ \nu_{12}^* = \nu_{21}^* = \nu^* &= \frac{\left(1-\frac{1}{R_k}\right)}{\left(1+\frac{3}{R_k}\right)} \\ G_{12}^* = G^* &= \frac{K_b}{b\sqrt{3}\left(1+\frac{2}{9R_k}\right)}. \end{aligned} \tag{13}$$

These expressions depend on the axial-to-bending stiffness ratio $R_k = R_{kh} = R_{kl}$, the bending stiffness $K_b = K_{bh} = K_{bl}$ and the depth of the network b. One observation of these expressions is that, despite the fact that there are only three effective elastic constants, the system is not isotropic since $G \neq \frac{E}{2(1+\nu)}$. The loss of isotropy results from the introduction of axial deformations

to the model. If the axial deformations are removed by setting $R_k \to \infty$ then the material becomes isotropic.

Figure 3 shows the variation of the effective properties with the axial-to-bending stiffness ratio R_k for $b = 4 \times 10^{-3}$ μm and $K_b = 6.3 \times 10^{-8}$, values representative of actin filaments. In each figure panel A shows the variation of the property over the full range of possible values, from the case in which axial deformations dominate for small R_k to the case in which axial deformations are negligible for large R_k. Panel B in each figure shows the variation of the properties only for $10^0 < R_k < 10^4$, the range of values obtained in physical systems. For physically realistic systems the elastic modulus varies by more than a factor of two with variation in R_k, the Poisson's ratio varies from 0 to 1, and the shear modulus is relatively insensitive to changes in R_k, showing a variation of only approximately 15% when R_k ranges from 10^0 to 10^4. In all cases most of the variation in the effective property occurs in the interval $10^0 < R_k < 10^2$.

The bending-normalized versions of Eqs. 13 are

$$\begin{aligned} E_1' = E_2' &= \left[1 + \frac{3}{R_k}\right]^{-1} \\ \nu_{12}' = \nu_{21}' &= \frac{1 - 1/R_k}{1 + 3/R_k} \\ G_{12}' &= \frac{1}{1 + 2/9R_k} \end{aligned} \tag{14}$$

These expressions depend only on the axial-to-bending stiffness ratio and the variation of these bending-normalized properties with R_k is shown in Fig. 4.

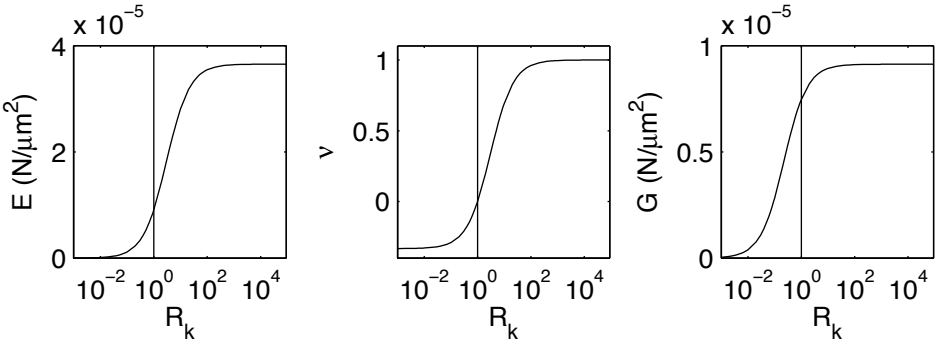

Figure 3: Variation of elastic properties with axial-to-bending stiffness ratio for regular hexagons. Regions to the right of the vertical line are realistic for physical structures.

Panel B of the figure shows clearly that the elastic modulus and Poisson's ratio can vary dramatically with changes in the axial-to-bending stiffness ratio in physically realistic cellular networks.

5.2 Rectangular unit cells

When the substitutions to obtain rectangular cells with identical cell walls are made to Eqns. 10 the expressions for the effective properties become

$$\begin{aligned} E_1^* &= \frac{R_k K_b}{b} = \frac{K_a}{b} \\ E_2^* &= \frac{K_b}{b\left(1+\frac{2}{R_k}\right)} \\ \nu_{12}^* = \nu_{21}^* &= 0 \\ G_{12}^* &= \frac{K_b}{b\left(3+\frac{1}{2R_k}\right)}. \end{aligned} \tag{15}$$

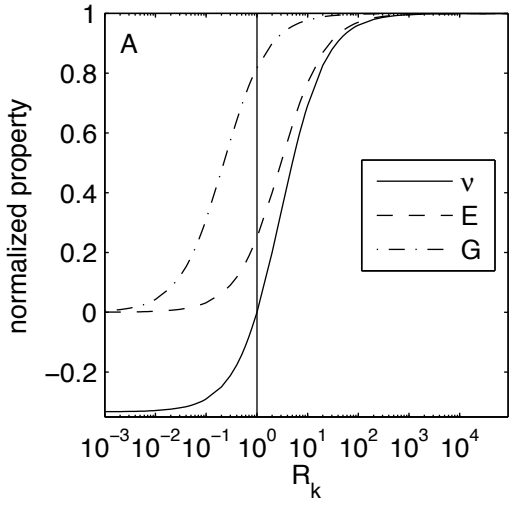

Figure 4: Variation of bending-normalized effective properties with axial-to-bending stiffness ratio for regular hexagons.

Here the material has different elastic stiffness in the two principal material directions and the material stiffness E_1^* is independent of the bending stiffness of the cell walls since no bending deformation occurs for loading in the x_1 direction with $\theta = 0$.

6 The role of relative density in determining cellular network properties

The relative density of cellular networks has typically been used as the single parameter used to predict mechanical properties, and therefore as the design parameter in material design. This section shows how the relative density and the axial-to-bending stiffness ratios are related and then shows, through

a numerical example, how cellular networks with the same density may have substantially different properties.

6.1 R_k relationship with density

Density is an important parameter in understanding cellular networks. Returning again to the simple (classical) case of networks of solid walls with rectangular cross-section, and using a low density approximation the normalized density $\rho_n = \rho^*/\rho_s$ is defined by (Eq. 4.1a in (5)):

$$\rho_n = \left(\frac{t/l(h/l+2)}{2cos(\theta)(h/L+sin(\theta))} \right). \tag{16}$$

substitution of the axial-to-bending stiffness ratios results in

$$\rho_n = \left(\frac{1/\sqrt{R_{kl}}(\sqrt{R_{kh}/R_{kl}}+2)}{2cos(\theta)(\sqrt{R_{kh}/R_{kl}}+sin(\theta))} \right). \tag{17}$$

For the special case of $h = l$ and $\theta = \pi/6$, then

$$\rho_n = \left(\frac{2}{\sqrt{3R_k}} \right). \tag{18}$$

which implies a limit of R_k between 4/3 and ∞ for this special network, and indicates that the density provides an alternative means to characterize the axial-to-bending stiffness ratio. However, as hollow cross-section are considered this relation is broken.

Now consider the density to stiffness relations for a network comprised

of hollow tubes, where ρ_s is defined as the density of the material making up the walls of the hollow tubes (which themselves comprise the walls of the network). In this case

$$\tilde{\rho}_n = \frac{\pi}{4}\sqrt{\frac{2}{3}}\frac{D}{D-1}\left(\frac{1/\sqrt{R_{kl}}(\sqrt{R_{kh}/R_{kl}}+2)}{2\cos(\theta)(\sqrt{R_{kh}/R_{kl}}+\sin(\theta))}\right) \tag{19}$$

where $\tilde{\rho}$ is a measure of the volume occupied cell walls, neglecting the fact that they may be hollow. If ρ'_s is defined as the density of the tubes (walls) themselves (noting that they are hollow, so $\rho'_s < 1$) then we may define ρ'_n which equals

$$\rho'_n = \frac{\rho^*}{\rho'_s} = \frac{\pi}{16}\sqrt{\frac{2}{3}}\frac{D^3}{D-1\sqrt{(D-1)^2+1}}\left(\frac{1/\sqrt{R_{kl}}(\sqrt{R_{kh}/R_{kl}}+2)}{2cos(\theta)(\sqrt{R_{kh}/R_{kl}}+sin(\theta))}\right). \tag{20}$$

The normalized density ρ'_n is a characterization of the actual density of material in the network while $\tilde{\rho}_n$ is a measure of the volume occupied by the cell walls, neglecting the fact that the cell wall members might be hollow; interestingly in the limit for a thin-walled tube as $D \to \infty$ ρ_n approaches a constant, but ρ'_n goes to ∞. For hollow cross-section members, unlike solid wall members, the d_o/t or D of the walls influences the $\rho - R_k$ relation and the limits of these expressions. The actual mass density of the cellular network $\rho_n\rho_s$ can be obtained by appropriate manipulation of the above relative densities.

6.2 Numerical example

Consider first a regular hexagonal cellular network with $l = h = 0.4\mu$m composed of a material with $E = 2.6 \times 10^{-3}\text{N}/\mu\text{m}^2$, and having cell wall members that are circular in cross section, and may be hollow. The cross section geometry is defined by the outer diameter d_0 and the wall thickness t. The diameter to thickness ratio D. The first cellular network considered here has $d_0 = 0.4\mu$m and $D = 100$. Recall that two different notions of relative density have been introduced. In one, the density of the network is normalized by the density of the cell wall. If the cell wall is not solid in cross section this wall-relative density, ρ_n' can exceed 1. The other definition of relative density follows that traditionally used in the analysis of networks with solid cell walls in which the cellular network density is normalized by the density of the solid material of which the network is composed. This relative density, the solid-relative density, is denoted here by ρ_n, and must fall in the interval $(0, 1]$.

For the cellular network described above, the wall-relative density is $\rho_n' = 2.29$ and the solid-relative density is $\rho_n = 0.0036$ and the stiffness ratio is $R_k = 68$. The solid-relative density is so low because the cell walls are composed of very thin-walled tubes. By holding the wall-relative density fixed it is calculated that a cellular network with $D = 50$ and $l = h = 0.185\mu$m has the same wall-relative density and an axial-to-bending stiffness ratio of $R_k = 18$. Similarly, by fixing the relative density one obtains a cellular network with $D = 2$, corresponding to a solid circular cross section, and

Table 2: Properties of cellular networks with constant relative density but varying axial-to-bending stiffness ratios

Property		Baseline $D = 100$, $l = 0.4$	Fixed ρ'_n $D = 50$, $l = 0.185$	Fixed ρ_n $D = 2$, $l = 10$
Stiffness ratio	R_k	68	18	85,000
Wall-rel. density	ρ'_n	2.3	2.3	3.6×10^{-3}
Rel. density	ρ_n	3.6×10^{-3}	0.014	3.6×10^{-3}
Solid-norm.	$\tilde{E}_1$	1.0×10^{-4}	1.8×10^{-3}	8.5×10^{-8}
Solid-norm.	$\tilde{\nu}_{12}$	0.94	0.80	1.0
Bending-norm.	E'_1	0.96	0.85	1.0
Bending-norm.	ν'_{12}	0.94	0.80	1.0

$l = h = 10\mu$m, with axial-to-bending stiffness ratio $R_k = 85,000$. In all calculations the thickness of the cellular network is taken to be $b = d_0 = 0.04\mu$m.

The bottom half of the table shows the elastic properties that are obtained for the three cellular networks described in the top half. The conclusion, seen by comparing, for example, the values of $\tilde{E}_1$ across the three columns, is that the properties of cellular networks can vary dramatically even when the density of the network is held constant. This conclusion opens the possibility of the design of cellular networks with a much broader range of properties than is possible if these properties are viewed as being tied closely to the network density.

7 Simulation of cellular networks

The expressions developed above give the effective orthotropic elastic properties of hexagonal cellular networks in which the cell walls have arbitrary

axial and bending stiffness. In this section these exact results are first compared to computational simulation of the elastic response of two dimensional model cellular networks. Then, simulation is used to examine the effect of uncertainty in the network geometry on the effective properties. Specifically, the vertices of a regular hexagonal cellular network are randomly perturbed to obtain cellular networks with random cell geometry. Cell wall section properties are held constant throughout the network, but, because the axial-to-bending stiffness ratios depend on cell wall length, these ratios vary element-by-element. Such random topologies cannot be analyzed using a unit cell approach, and so Monte Carlo simulation of the response of these random cellular networks is used to examine the distribution of effective properties and compare to the properties of a regular hexagonal cellular network in which the cell walls have identical cross sectional properties.

In all the simulations described in this section the cell walls are modeled by Euler-Bernoulli beam elements, with one element used per cell wall, all connections are moment connections, and calculations are performed by the commercial finite element package `ABAQUS` (1).

7.1 Ordered cellular networks

The geometry of the samples used in the computational simulation of the response of ordered cellular networks are composed of regular hexagons with $h = l$, $\theta = \pi/6$, $I_h = I_l$, and $A_h = A_l$. The samples analyzed are roughly square, and consist of n_1 cells in the x_1 direction and n_2 cells in the x_2 di-

rection. Uniaxial extension is imposed by displacement boundary conditions in which the lateral edges are left free.

The comparison presented here is between the bending-normalized effective properties calculated from Eqs. 14 and the same properties estimated from computational simulation. The properties used in simulation of the ordered cellular networks are given in Table 3 in units of Newtons and microns. The properties in the column labeled 'case I' represent those of a typical actin filament found in the cytoskeleton. The properties in the column labeled 'case II" are identical to those for case I except that the cross sectional area has been reduced by a factor of 100. This is done to provide a range of values of the axial-to-bending stiffness ratio R_k, namely $R_k = 123$ for case I and $R_k = 1.23$ for case II.

Calculation of the bending-normalized effective properties requires the value of the properties when only bending deformations are included. To obtain these values the cross sectional area of the cell walls is increased so that the axial compliance of the cell walls approaches zero, thereby eliminating axial deformations from the simulation. The properties used in these simulations are also given in Table 3. The value of the cross sectional area chosen to eliminate axial deformations is determined from a convergence study since excessively large values of the cross sectional area can lead to numerical instability in the linear elastic finite element analysis. The axial-to-bending stiffness ratio value of 10,000 that is used to eliminate axial deformation is well into the range of values where the contribution of axial compliance to

Table 3: Properties of actin filaments used in simulation of ordered cellular networks

Property	case I	case II	high R_k
$E(N/\mu\text{m}^2)$	2.6×10^{-3}	2.6×10^{-3}	2.6×10^{-3}
A_h, A_l (μm^2)	12×10^{-4}	12×10^{-6}	1×10^{-1}
I_h, I_l (μm^4)	13×10^{-8}	13×10^{-8}	13×10^{-8}
l_h, l_l (μm)	0.40	0.40	0.40
R_{kh}, R_{kl}	123	1.23	10,000

Table 4: Comparison of exact and simulated effective properties for regular hexagonal honeycomb

Bending-normalized property	Exact I	Simulated I	Exact II	Simulated II
E'_1 (N/μm^2)	0.98	0.98	0.29	0.29
E'_2 (N/μm^2)	0.98	0.98	0.29	0.29
ν'_{12}	0.99	0.97	0.054	0.057
ν'_{21}	0.99	0.97	0.054	0.057

total compliance of the network is negligible (See Figs. 3-4).

The effective properties of the cellular networks as estimated from the simulations are sensitive to the size of the network modeled, and show convergence as the number of cells increases. The effective properties are well converged when the size of the simulated honeycomb is $n_1 = n_2 = 100$. The results of simulations at this honeycomb size are shown in Table 4 and show excellent agreement between the predictions and simulations. The agreement is somewhat better in the predicted elastic moduli than the Poisson's ratios, but the worst error is approximately 5%.

7.2 Irregular cellular networks

Examples of cellular networks with random cell geometry exist in naturally occurring and engineered systems, such as cancellous bone, the network of

actin filaments in a cell, foamed metals, and space frames. This subsection describes numerical simulation used to evaluate the propagation of uncertainty in the shape of the cells of a two dimensional cellular network to uncertainty in the effective elastic properties. Monte Carlo simulation of irregular cellular networks is used to estimate the statistical moments and distribution of the effective properties. It is important to note at this point that uncertainty in the effective properties of irregular networks has two sources, the irregularity of the shape, and the variability in the axial-to-bending stiffness ratio introduced by variability in the edge length of the cells.

For the irregular networks analyzed here the cross sectional properties of the cell walls are deterministic. As for the regular networks, two cases are investigated for which the cross sectional properties are given in Table 3. The irregularity of the cells, however, makes the cell wall length a random variable.

Here, irregular networks are generated by perturbing the location of the vertices of a regular cellular network. Denoting the position of a vertex by v, the location of this vertex in the perturbed, irregular, network, is given by

$$\hat{v} = v + \alpha u \frac{h + l}{2} \tag{21}$$

in which u is a vector whose components are independent and uniformly distributed in the interval $[-0.5, 0.5]$, and α is the magnitude of the perturbation scaled by the average of the cell wall lengths h and l. Figure 5 shows two

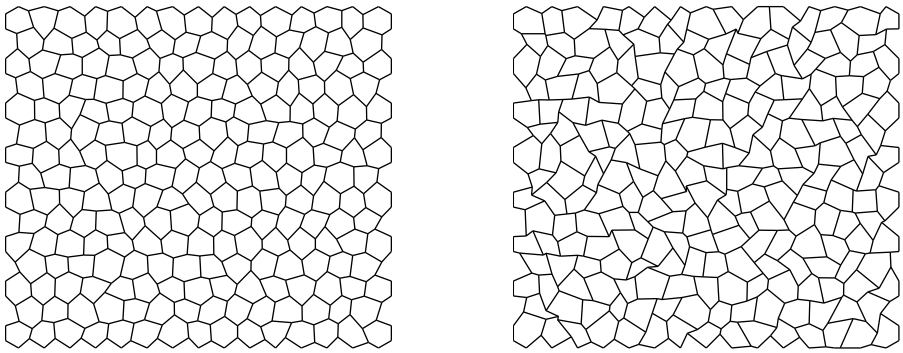

Figure 5: Irregular hexagonal cellular networks generated by perturbation of regular hexagonal cellular networks with perturbation magnitudes of (A) $\alpha = 0.5$ and (B) $\alpha = 1.0$.

example perturbed hexagonal cellular networks both with $n_1 = n_2 = 25$ and with $\alpha = 0.5$ and $\alpha = 1.0$. In the perturbed hexagonal networks vertices on the boundaries are not perturbed. This is done to ease the application of the boundary conditions in the numerical simulations and does not substantially affect the response of the network. When the magnitude of the perturbation becomes large, as shown in part (B) of the figure, cells can become concave. This may have substantial effect on the effective properties of the network.

The expressions developed for the effective properties of regular cellular networks depend on the axial-to-bending stiffness ratios, the side lengths, and the angle θ, all of which become random in the perturbed hexagonal cellular networks. Figure 6 shows histograms of the edge length for a network with approximately 2,500 cells, the properties of case II of Table 3 and $\alpha = 0.5$ or $\alpha = 1.0$. Figure 7 shows a comparison of the axial-to-bending stiffness

ratios R_k for the same perturbed hexagonal networks. Two key observations from these results are that the mean edge length is increased above 0.4 μm by perturbation of the vertices, and that the mean of the axial-to-bending stiffness ratio, for the case $\alpha = 1.0$, has been increased by 30% over the value of 1.23 obtained for the case II regular hexagonal cellular network. The distribution of the axial-to-bending stiffness ratio also acquires significant positive skewness during the process of vertex perturbation. For both cases the mean cell wall length is longer than the edge length of 0.4 μm that prevails in the ordered hexagonal networks. The increase in the mean cell wall length is small, 2.5% for $\alpha = 0.5$ and 7.5% for $\alpha = 1.0$., yet the resulting increases in the average axial-to-bending stiffness ratio are 6% for $\alpha = 0.5$ and 30% for $\alpha = 1.0$. The larger increase in the axial-to-bending stiffness ratio is due to the dependence of the axial-to-bending stiffness ratio on the square of the cell wall length (see Eqs. 3)

The results of 100 simulations of the deformation of perturbed hexagonal cellular networks with $\alpha = 0.5$ and $\alpha = 1.0$ are summarized in Table 5. For both sets of simulations the cross section properties of the cell walls are drawn from the column labeled case II of Table 3. The results show that the bending-normalized stiffness of the networks is reduced slightly, by 7% for $\alpha = 0.5$ and by 17% for $\alpha = 1.0$, and that the bending-normalized Poisson's ratio is approximately doubled, when compared to the values obtained for a regular hexagonal cellular network with edge length $h = l = 0.4\mu$m. The column in the table labeled 'predicted' shows the properties that would be

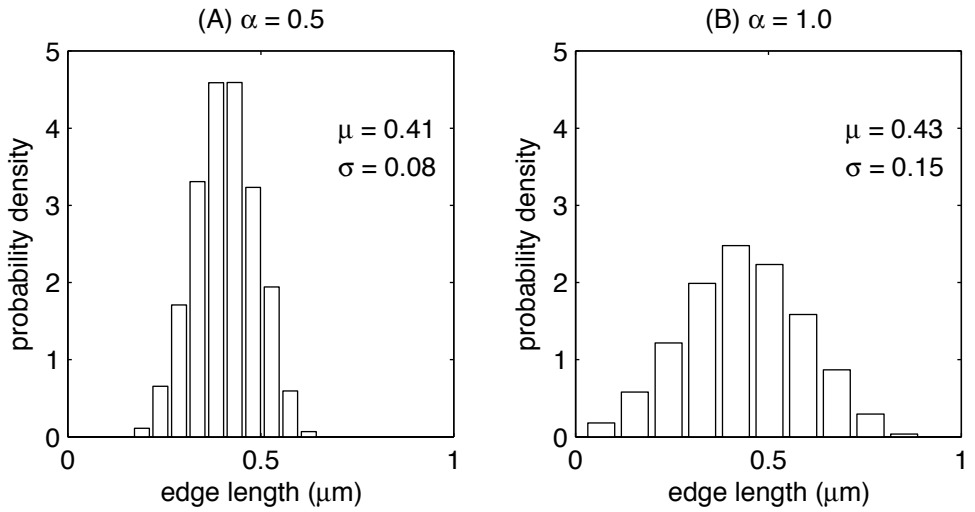

Figure 6: Histograms of edge length for perturbed hexagonal cellular networks with (A) $\alpha = 0.5$ and (B) $\alpha = 1.0$.

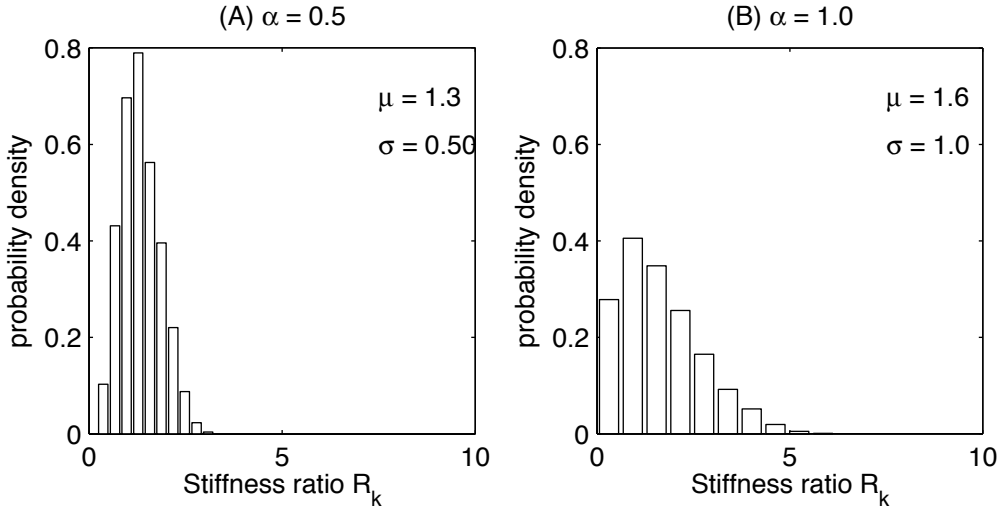

Figure 7: Histograms of axial-to-bending stiffness ratio for perturbed hexagonal cellular networks with (A) $\alpha = 0.5$ and (B) $\alpha = 1.0$.

Table 5: Simulated effective properties of perturbed hexagonal cellular networks.

		$\alpha = 0.5$			$\alpha = 1.0$	
Property	mean	st. dev.	predicted	mean	st. dev.	predicted
Bending-norm.						
E_1'	0.27	0.0019	0.30	0.24	0.0056	0.35
E_2'	0.27	0.0019	0.30	0.25	0.0046	0.35
ν_{12}'	0.096	0.0014	0.070	0.22	0.0055	0.13
ν_{21}'	0.094	0.0019	0.070	0.22	0.0040	0.13
Solid-norm.						
E_1^*	3.8×10^{-4}	5.8×10^{-7}	4.0×10^{-4}	3.3×10^{-4}	1.7×10^{-6}	3.9×10^{-4}
E_2^*	3.8×10^{-4}	1.5×10^{-6}	4.0×10^{-4}	3.3×10^{-4}	2.6×10^{-6}	3.9×10^{-4}
ν_{12}^*	0.086	0.0019	0.070	0.14	0.0033	.13
ν_{21}^*	0.086	0.0013	0.070	0.14	0.0024	.13

obtained from Eqs. 14 using the mean cell wall length for the disordered hexagonal networks. The thickness of the network has been assumed to be $b = 0.4\mu$m The computed bending-normalized stiffness is 23% less than predicted for $\alpha = 0.5$ and 31% less than predicted for $\alpha = 1.0$. The properties of a disordered cellular network cannot be predicted merely by substituting the mean axial-to-bending stiffness ratio into Eqs. 14, disorder tends to reduce the stiffness of the cellular networks, and an increase in disorder leads to a greater decrease in stiffness. The results also show that the properties in the two principal material directions are equal and that the network size used here, $n_1 = n_2 = 50$, is a representative volume element in which the variability of the properties from sample to sample is small.

8 Conclusions

Cellular networks underly a large variety of natural and man-made materials and systems. The mechanical response of such networks is of great interest both from the perspective of understanding and predicting their response, as well as designing a particular desired elastic response. Herein the effective elastic properties of periodic cellular networks are derived as a function of the axial-to-bending stiffness ratio of the cell walls. The effective properties vary significantly as a function of the axial-to-bending stiffness ratio, e.g. Poisson's ratio may vary from near zero to near one in physically realizable networks as a function of the axial-to-bending stiffness ratio. Further, due to the contribution from axial deformations, knowledge of the density alone is not adequate for predicting the structural response of the network. Finite element simulations of an ordered cellular network composed of actin filaments agree well with the analytical expressions. Finite element simulations of dis-ordered (perturbed) cellular networks show that such networks have properties that differ substantially from those that would be predicted for a topologically equivalent ordered cellular network. Specifically, disorder in the network topology tends to soften the material response. The refinements introduced in this paper have particular relevance to current developments in materials design, in which cellular and truss-like networks are being constructed with hollow cell walls. Finally, it is emphasized that the notion of a cellular network as a structural system is applicable across a very broad range of

length scales, from nano-scale carbon nanotubes to the macroscale structural steel buildings, towers, and space frames.

Acknowledgments

Johns Hokpins University graduate student Mina Seif contributed to initial calculations related in part to this paper. The second author would also like to recognize the partial financial support provided through the Howard Hughes Medical Institute NBMed Graduate Training Program at Johns Hopkins University. The work was partially supported by the US National Science Foundation through grants NSF CMMI-1000334, 1000167, 0970059.

References

[1] Abaqus. *Abaqus/Standard User's Manual, version 6.3*. Simulia, Pawtucket, RI, 2002.

[2] AISC. *Steel Construction Manual*. American Institute of Steel Construction, Chicago, IL, 2005.

[3] E. Andrews, W. Sanders, and L.J. Gibson. Compressive and tensile behaviour of aluminum foams. *Materials Science & Engineering*, A270-2:113–124, 1999.

[4] S. R. Arwade and M. Grigoriu. Characterization and modelling of ran-

dom polycrystalline microstructrues with application to intergranular fracture. *Journal of Engineering Mechanics*, 130:997–1006, 2004.

[5] L. Gibson and M. F. Ashby. *Cellular Solids: structure and properties*. Cambridge University Press, Cambridge, England, 1997.

[6] L. Gong, S. Kyriakides, and W.-J. Jang. Compressive response of open cell foams. part i: Morphology and elastic properties. *International Journal of Solids and Structures*, 42:355–1379, 2005.

[7] W.-Y. Jang, A.M. Kraynik, and S. Kyriakides. On the microstructure of open cell foams and its effect on elastic properties. *International Journal of Solids and Structures*, 45:1845–1875, 2008.

[8] H. Liu, S. R. Arwade, and T. Igusa. Random composites classication and damage estimation using bayesian classiers. *Journal of Engineering Mechanics*, 133:129–140, 2007.

[9] M.H. Luxner, J. Stampfl, and H.E. Petterman. Numerical simulations of 3d open cell structures — influence of structural irregularities on elasto-plasticity and deformation localization. *International Journal of Solids and Structures*, 44:2990–3003, 2007.

[10] M. Meo and M. Rossi. A molecular-mechanics based finite element model for strength prediction of single wall carbon nanotubes. *Materials Science & Engineering*, A 454-455:170–177, 2007.

[11] S.D. Papka. In-plane compressive response and crushing of honeycomb. *Journal of the Mechanics and Physics of Solids*, 42:1499–1532, 1994.

[12] S.D. Papka and S. Kyriakides. Experiments and full scale numerical simulations of in plane crushing of a honeycomb. *Acta Materialia*, 46:2765–2776, 1998.

[13] S.D. Papka and S. Kyriakides. In plane crushing of a polycarbonate honeycomb. *International Journal of Solids and Structures*, 35:239–267, 1998.

[14] B. W. Schafer. Review: The direct strength method of cold-formed steel member design. *Journal of Constructional Steel Research*, 64:766–778, 2008.

[15] B. W. Schafer and S. R. Arwade. Mechanical properties of random networks. In *Proceedings of the 17th ASCE Engineering Mechanics Conference*, Newark, DE, 2004. ASCE.

[16] Matthew J Silva, Wilson C. Hayes, and Lorna J Gobson. The effect of non-periodic microstructure on the elastic properties of two dimensional cellular solids. *International Journal of Mechanical Sciences*, 37:1161–1177, 1995.

[17] M.J. Silva and L.J. Gibson. The effects of non periodic microstructure and defects on the compressive strength of two-dimensional cellular solids. *International Journal of Mechanical Sciences*, 39:549–563, 1997.

[18] L. Tan and S. R. Arwade. Response classication of simple polycrystalline microstructures. *Computer Methods in Applied Mechanics and Engineering*, 197:1397–1409, 2008.

[19] Y. Tseng, T. P. Kole, B. W. Schafer, E. Feorov, S. C. Almo, and D. Wirtz. How actin crosslinking proteins cooperate to generate an enhanced cell mechanical response. *Journal of Cell Biology*, 334:183–192, 2004.

[20] W.E. Warren and A.M. Kraynik. Foam mechanics: the linear elastic response of two dimensional spatially periodic cellular materials. *Mechanics of Materials*, 6:27–37, 1987.

[21] W.E. Warren and A.M. Kraynik. Linear elastic behavior of a low-density kelvin foam with open cells. *Journal of Applied Mechanics*, 64:787–794, 1997.

[22] N. Wicks and J. W. Hutchinson. Optimal truss plates. *International Journal of Solids and Structures*, 38:5165–5183, 2001.